The Institute of Space and Astronautical Science
Report SP No. 17 March 2003

Rarefied Aerodynamics of MUSES-C Sample Return Capsule

By

Kazuhisa FUJITA*, Yoshifumi INATANI*, Kojyu HIRAKI*, and Takashi ABE*

(1 February 2003)

Abstract: Dynamics stability of the MUSES-C sample return capsule has been assessed in the rarefied gas environments, from the free-molecular to transitional regime. Overall aerodynamic coefficients were determined by the empirical bridging method, and their accuracy was validated by a three-dimensional DSMC analysis of rarefied flows around the capsule. To obtain realistic aerodynamic coefficients in the DSMC analysis, nonequilibrium thermal relaxation and chemical kinetics were incorporated into the numerical model. The aerodynamic coefficients determined by the empirical formula are found to be in good agreement with those obtained by DSMC calculations. Rarefaction of the flow and position of the center of gravity of the capsule are found to have significant influences on pitching stability of the capsule. The six-degrees-of-freedom dynamics of the capsule was numerically simulated along the reentry trajectory to examine the effect of spin frequencies on stability of the capsule.

1. INTRODUCTION

Hypersonic vehicles reentering the earth atmosphere experience a wide range of gas density, from the rarefied to dense gas environments along their flight trajectory. As the gas density decreases, rarefaction of flows around the vehicle becomes to have considerable influences on the aerodynamic characteristics of the vehicle. In particular, such effects on the pitching moment are significant since the pitching moment acting on the vehicle plays a major role in stabilizing the attitude of the vehicle. Disk-shaped reentry capsules that are frequently used in these days are designed to maintain static and dynamic stability in hypersonic flight when the flow around the capsule can be regarded to be continuous. However, the stability of such capsules is in general degraded as the flow becomes rarefied. To take the STARDUST sample return capsule of NASA as an example, the pitching moment coefficient becomes positive for positive angles of attack as the Knudsen number decreases below 0.1 (Wilmoth et al. (1997)). Consequently, the capsule is expected to tumble during reentry unless the spin stabilization is used in the initial phase of reentry operation.

* The Institute of Space and Astronautical Science, 3-1-1, Yoshinodai, Sagamihara, Kanagawa 229-8510, Japan.

Similar instability due to rarefaction of the flow is considered to occur to the sample return capsule of the MUSES-C mission programmed by ISAS, since it has a disk-shaped form similar to the STARDUST capsule. In comparison with the STARDUST capsule, the instability is expected to be less significant because 1) the MUSES-C capsule has a smaller aftbody in proportion to the forebody, and 2) the center of gravity is located more afore in proportion to the axial total length of the capsule. However, in order to examine whether the capsule finally tumbles or not during reentry, it is necessary to perform a detailed analysis of the capsule dynamics along the flight trajectory since the capsule dynamics is much affected by the initial conditions of reentry such as the angle of attack and spin frequency.

In this article, numerical analyses have been performed to assess the dynamic stability of the MUSES-C capsule in the rarefied gas environments, from the free-molecular to transitional regime. In Sec. 2, overall aerodynamic coefficients are determined by the empirical bridging method, using the aerodynamic coefficients for the continuous and free-molecular gas environments. Accuracy of the transitional aerodynamic coefficients are validated by a three-dimensional DSMC analysis of rarefied flows around the capsule in Sec. 3. The capsule dynamics is examined in Sec. 4 by a six-degrees-of-freedom analysis along the reentry trajectory.

2. AERODYNAMIC COEFFICIENTS VIA BRIDGING FORMULA

The aerodynamic coefficients such as the axial and normal coefficients (C_A and C_N, respectively) and the pitching moment coefficient (C_m) for continuous flows were obtained by the wind tunnel measurements in the subsonic to supersonic conditions (M=0.3 to 4.0 where M is the Mach number), and by the computational fluid dynamic analysis up to $M = 8$ (Hiraki (2002)). The aerodynamic coefficients for free-molecular flows were determined by the geometrical particle-tracing analysis. In this calculation, the accommodation factor for particles reflection on the capsule surface was set to be unity, that is, completely diffusive reflection was assumed since this was found to give a conservative estimation of the pitching moment coefficients.

The transitional aerodynamic coefficients between the free-molecular and continuous flow conditions were determined by the standard sine-squared relation (Blanchard et al. (1986)), which is an empirical formula to calculate the transitional aerodynamic coefficients from the aerodynamic coefficients in the free-molecular and continuum limits as a function of the Knudsen number. In the present analysis, the bridging relation was given as

$$C = C_c + C_f \sin^2\left[\frac{\pi}{8}\left(3 + \log_{10} K_n\right)\right] \tag{1}$$

where C is the bridged aerodynamic coefficient (C_A, C_N, and C_m), subscripts c and f refer to the value in the free-molecular and continuum limits, respectively, and K_n is the Knudsen number. Typical examples of the overall aerodynamic coefficients obtained above are shown in Figs. 1 and 2 as solid lines. The angle of attach is defined as the angle between the direction of flight and the center axis of the capsule and denoted as A/A hereafter. In Figs. 1 b) and 2, X_c is the distance of the center of gravity of the capsule measured from the forefront. The aerodynamic coefficients shown in Fig. 1 are the results for A/A = 20 deg. C_m is plotted for X_c = 0.10, 0.11, 0.12, and 0.13 m in Fig. 1 b), while variation of C_m along with A/A is illustrated in Fig. 2 for several flight altitudes in the case of X_c = 0.13 m.

The Knudsen number is defined by using the capsule diameter as the representative length, which is 0.404 m for the MUSES-C capsule. In Fig. 1, the influences of flow rarefaction become

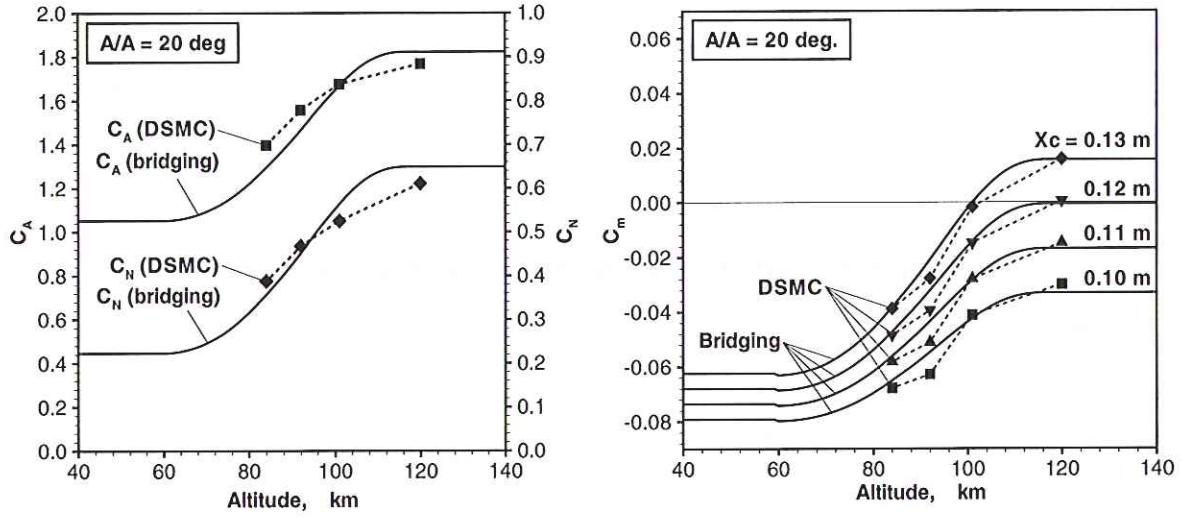

a) Axial and normal coefficients b) Pitching moment coefficient

Fig. 1: Overall aerodynamic coefficient of MUSES-C capsule : obtained by empirical bridging formula ; angles of attack = 20 deg.

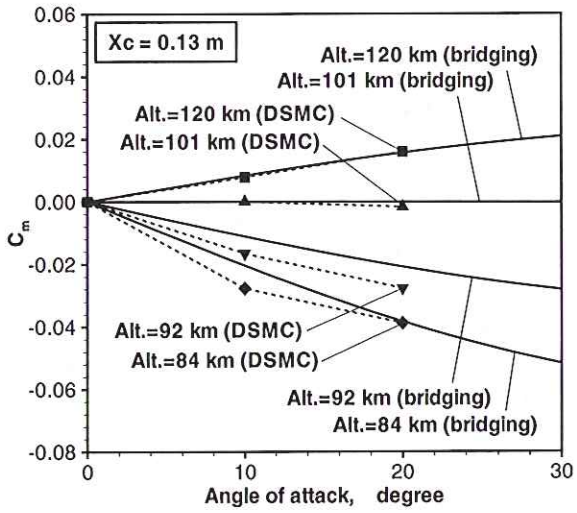

Fig. 2: Pitching moment coefficient as a function of angle of attack.

noticeable as the flight altitude increases above 80 km ($K_n > 0.01$), and the flow around the capsule can be regarded to be in the free-molecular condition above 110 km ($K_n > 1$). C_A and C_N increase by the factor of approximately 2 from the continuous to free-molecular condition. In particular, C_m increases as the flow is rarefied ; though C_m remains negative, $|C_m|$ decreases for $X_c < 0.12$ m, while C_m becomes positive for $X_c > 0.12$ m as the flight altitude increases. This brings about static instability of the capsule about the pitching movement.

In Wilmoth et al. (1997), C_m of the STARDUST capsule was estimated to be 0.03 for A/A = 10 deg. in the free-molecular condition, while that of the MUSES-C capsule is 0.01 for the same angle of attack with $X_c = 0.13$ m. Therefore, the pitching instability induced by flow

rarefaction is expected to be less significant for the MUSES-C capsule than the STARDUST capsule. However, as seen in Figs. 1 and 2, the pitching instability is very sensitive to position of the center of gravity (or X_c) in transitional to free-molecular flows. For this reason, in the following part of this article, accuracy of the aerodynamic coefficients obtained by the empirical bridging formula are validated by a three-dimensional DSMC analysis of rarefied flows around the capsule.

3. AERODYNAMIC COEFFICIENTS VIA DSMC ANALYSIS

3.1 DSMC Model

The DSMC computer code used in the present analysis is RARAC-3D (rarefied and reacting air flow calculation code for 3-dimensional geometries) developed by the author for the present study. Using RARAC-3D, rarefied air flows in thermal and chemical nonequilibrium conditions can be computed in arbitrary three dimensional geometries. Since ionization seldom occurs in comparison with dissociation and recombination of molecular species in the rarefied environments under consideration, N_2, O_2, N, O, and NO are currently taken into account as the gas components.

In RARAC-3D, elastic collision cross-sections are computed by using the variable hard sphere (VHS) model developed by Bird (1981). The adjusting parameters of the VHS model for collisions between the same collision partners are derived from the viscosity coefficients of pure gases. On the other hand, the VHS parameters for collisions between different collision partners are determined from the binary diffusion coefficients, following the method of Nanbu (1990). To determine the VHS parameters in RARAC-3D, the viscosity and binary diffusion coefficients were computed by using the collision integrals given recently by Capitelli et al. (1998).

In order to assess the aerodynamic coefficient accurately, it is necessary to take into account the effects of nonequilibrium thermal relaxation and chemical kinetics which may occur in the flow around the capsule. Both phenomena have significant influences on translational temperature and density distributions in the flow, and consequently, on the pressure distribution around the capsule. In RARAC-3D, relaxation of the molecular rotational mode is computed by using the translational-rotational energy-exchange probabilities of Boyd (1990). The adjusting parameters in the Boyd model were determined from the rotational collision number of Parker (1959). Since the Parker model has been validated by experiments only at low temperatures below several thousands K, its accuracy at higher temperatures is an open question (Lumpkin et al. (1989)). Recent quasi-classical trajectory calculations (for example, Fujita et al. (2002)) give the rotational state-to-state rate coefficients at high translational temperatures up to 90,000 K, and suggest that the Parker model can be a good approximation for translational-rotational energy exchange even at higher temperatures.

On the other hand, relaxation of the molecular vibrational mode is computed by using translational-vibrational energy-exchange probabilities determined from the macroscopic vibrational relaxation time of Park (1993). In this approximation, the energy-exchange probability is given at each computational cell as a cell-averaged value, which depends only on the translational temperature determined in each cell. In inelastic collisions where the translational-rotational and translational-vibrational energy exchange take place, the ratio of energy redistribution among the translational, rotational, and vibrational modes is computed by the Borgnakke-Larsen phenomenological model (Borgnakke et al. (1975)).

Chemical reactions incorporated into the present 5-species air model are summarized in

Table 1: Chemical reactions taken into consideration.

	Reactions	Reaction rates
1)	$N_2 + M^a \leftrightarrow 2\,N + M$	Park (1993)
2)	$O_2 + M \leftrightarrow 2\,N + M$	Park (1993)
3)	$N_2 + O \leftrightarrow N + NO$	Park (1993)
4)	$O_2 + N \leftrightarrow O + NO$	Park (1993)
5)	$NO + M \leftrightarrow N + O + M$	Park (1993)

[a] M = N_2, O_2, N, O, or NO. The reaction rate is subject to M.

Table 1. In RARAC-3D, probabilities of two-body reactions, i.e, the forward reactions of 1) to 5) and the backward reactions of 3) and 4) are calculated by the method of Bird (1979), while those of three-body reactions, i.e, the backward reactions of 1), 2), and 5) are determined by the method of Boyd (1990). In both methods, the reaction probabilities are determined from the corresponding Arrhenius-type reaction rate coefficients given by Park (1993).

In RARAC-3D, DSMC calculations are performed by the maximum-collision-number algorithm developed by Nanbu (1992). Rectangular parallelepiped cells are used to reduce the computational time required to index the test particles in the DSMC algorithm. In order to capture steep changes of physical properties in the vicinity of capsule surface and in the shock wave, a solution-adaptive grid-reconstruction technique is used during the time-marching computation ; a computational cell having the Knudsen number less than unity is divided into eight child cells of the same dimension (i.e., divided into halves in the x, y, and z direction). Conversely, if the cell Knudsen numbers of eight child cells are all greater than unity, the eight child cells are reunited into the original parent cell. Such a procedure is repeated at every 1,000 iterative step of time-marching computation until the flow approaches a steady state asymptotically. The grid system obtained finally for the flight altitude of 92 km and A/A = 10 deg. is shown in Fig. 3 as an example. In Fig. 3, computational cells on the plane of symmetry are only illustrated.

In the present DSMC analysis, particles impinging on the capsule surface were assumed to be reflected in the completely diffusive manner, since the free-molecular aerodynamic coefficients were calculated also with this assumption to obtain a conservative estimation of the pitching moment coefficient. The wall temperature (T_W) of the capsule was assumed to be 500 K uniquely. In reality, since the free stream velocity is very high in the flight environments of the MUSES-C capsule, the aerodynamic coefficients were found to be independent of T_W as far as T_W remains below 2,000 K. The assumption of $T_W < 2,000$ K is considered to be reasonable for flight altitudes tested in the present DSMC analysis, which are 84 km and above, since the aerodynamic heating of the capsule is not expected to be significant at these altitudes.

3.2 Numerical Results

DSMC calculations were performed for four flow conditions along the reentry trajectory, which are summarized in Table 2. In each case, we calculated flows for three angles of attack, 0, 10, and 20 deg. The aerodynamic coefficients were determined from the ensemble average of momenta transferred from test particles to the capsule surface. As a typical example, distributions of particles number density and translational temperature for A/A = 20 deg. are shown in Figs. 4

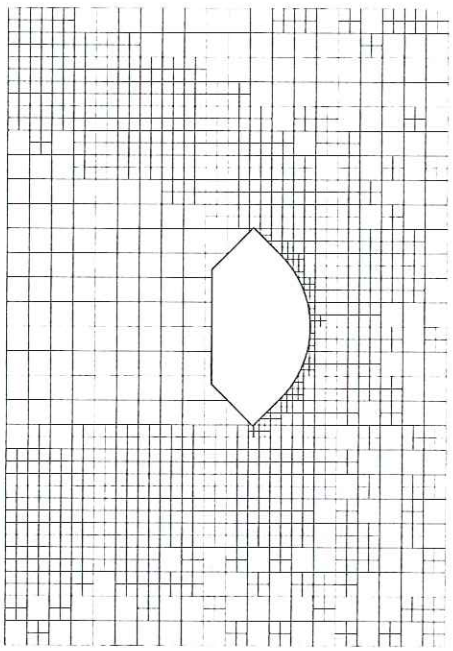

Fig. 3: Solution-adaptive grid based on cell Knudsen number : on symmetric plane, altitude = 92 km.

Table 2: Flow conditions tested in DSMC analysis.

Case	Altitude (km)	Velocity (km/s)	Temperature (K)	Pressure (Pa)	K_n	Mole concentration		
						N_2	O_2	O
a)	120	12.26	394.7	0.002994	5.6	0.7327	0.1828	0.0845
b)	101	12.28	193.3	0.02526	0.66	0.7844	0.1768	0.0388
c)	92	12.28	187.9	0.1349	0.12	0.7873	0.2056	0.0071
d)	84	12.27	201.0	0.6769	0.025	0.7615	0.2385	0

and 5, respectively.

The flow around the capsule is a free-molecular flow in Case a), since the Knudsen number is much greater than unity. On the other hand, the flow is close to continuum in Case d) because the Knudsen number is only slightly larger than 0.01. As the flight altitude increases and the density decreases accordingly, the bow shock around of the capsule becomes less distinct and the shock stand-off distance increases. Conversely, as the density increases, collisions among molecules become to occur more frequently, and the translational energy is more transferred to other internal energy modes and consumed to dissociate molecules, resulting in a decrease of the translational temperature, as seen in Fig. 5.

The aerodynamic coefficients obtained by the DSMC calculations are plotted in Figs. 1 and 2 as close symbols with dashed lines. In general, the aerodynamic coefficients determined by the empirical formula (shown as solid lines) are in good agreement with the DSMC aerodynamic coefficients; differences in C_A and C_N between the empirical and DSMC calculations remains less than 10%. Considering the errors originating from the ensemble average and the

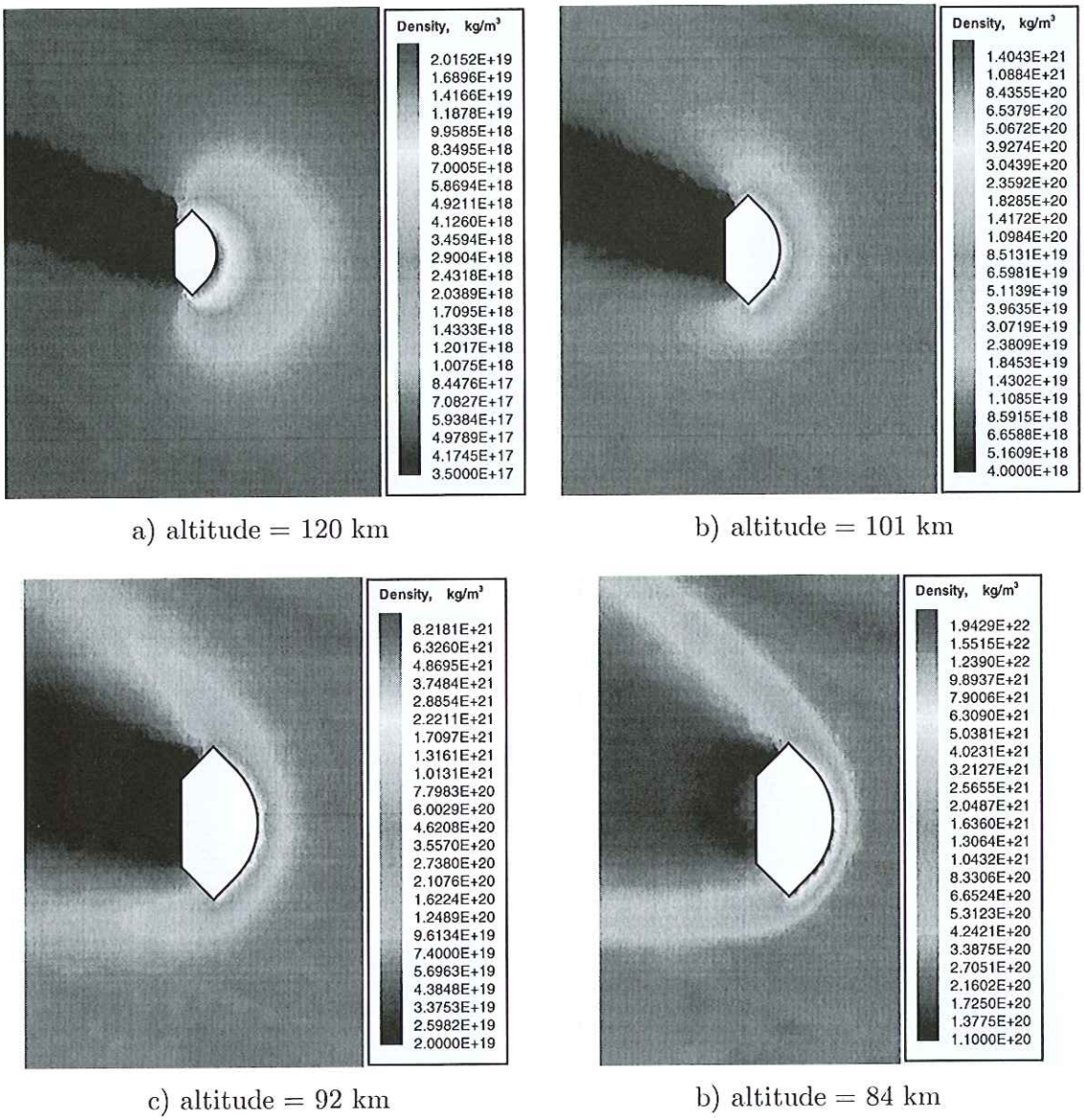

a) altitude = 120 km

b) altitude = 101 km

c) altitude = 92 km

b) altitude = 84 km

Fig. 4: Total density distribution around the MUSES-C capsule : A/A = 20 deg.

uncertainties involved in the thermal relaxation models and the chemical reaction rate coefficients in the DSMC analysis, only the 10% differences between the two results obtained by different approaches suggest that the empirical bridging formula defined by Eq. (1) can be a good approximation for the MUSES-C capsule.

4. DYNAMICS OF MUSES-C CAPSULE ALONG REENTRY TRAJECTORY

In this section, dynamics of the MUSES-C capsule is numerically analyzed in the free-molecular to continuous gas environments along the reentry trajectory to assess the dynamic stability of the capsule during hypersonic flight. All of the six degrees of freedom of capsule motion are taken into consideration, so that the effect of spin stabilization on the capsule dynamics can be examined accurately. The geodetic reference system 1980 (GRS80) is used to represent

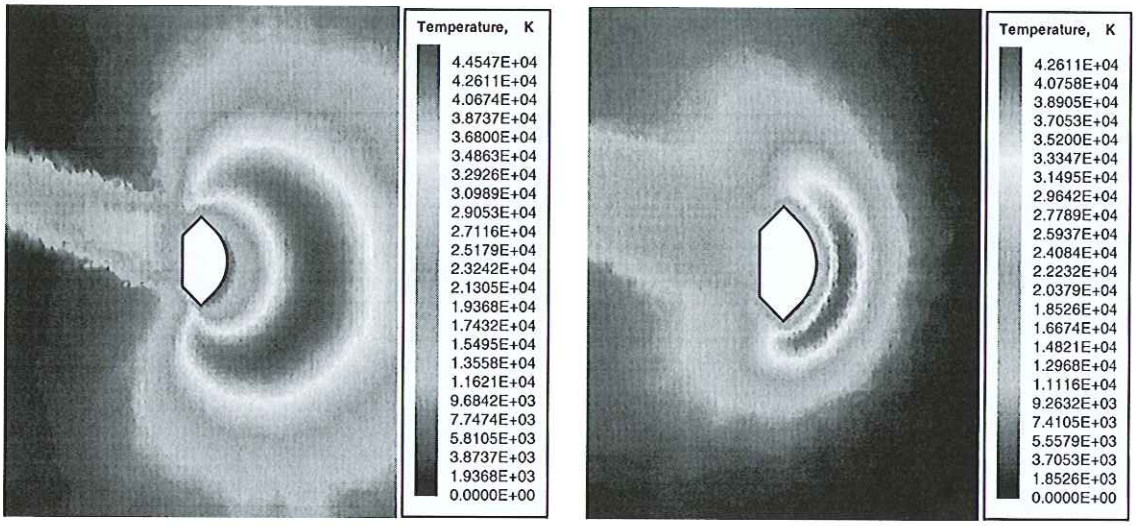

a) altitude = 120 km b) altitude = 101 km

c) altitude = 92 km d) altitude = 84 km

Fig. 5: Translational temperature distribution around the MUSES-C capsule : A/A = 20 deg.

the surface of earth. On the other hand, the NASA/MSFC global reference atmosphere model 1995 version (GRAM95; Justus et al. (1995)) is used without taking into account the effects of wind and dispersion in atmospheric density.

The initial conditions of reentry are summarized in Table 3. In order to perform conservative simulations of the capsule dynamics, the initial angle of attack is assumed to be 10 deg. In reality, the pointing direction of the capsule can be controlled much more accurately at separation from the satellite in the nominal reentry operation. Initial nutation is neglected since it is considered to be very small, while the roll damping coefficient is constantly given as $C_{lp} = -0.01$. The overall aerodynamic coefficients obtained by the empirical bridging method are used, since they are continuously defined over a wide range of the Knudsen number, and since they are considered to maintain moderate accuracy in the transitional environments as

Table 3: Initial conditions for reentry of MUSES-C capsule.

geometric altitude (km)	geometric latitude (deg)	geometric longitude (deg)	relative velocity (km/s)	flight path angle (deg)	flight azimuthal angle (deg)
204.6	−28.22	126.64	11.96	−12.85	114.99

validated above by the DSMC analysis.

Time evolution of A/A is illustrated in Figs. 6 a) to d) for different positions of the center of gravity. The notations A/A (0 Hz) and A/A (0.1 Hz) given in the figures represent the results in which the initial spin frequencies denoted between parentheses are prescribed, respectively. As seen in Fig. 1 b), C_m remains negative regardless of the flight altitude for $X_c < 0.12$ m. For this reason, the pitching moment acting on the capsule always works to decrease the angle of attack for $X_c = 0.10$ m, as seen in Fig. 6 a). Without spin, the angle of attack decreases and the pitching motion damps down along the flight trajectory. When initial spin is given to the capsule, since the pitching motion is restricted to the spin axis, A/A does not decreases until the aerodynamic force acting on the capsule becomes strong in accordance with an increase of gas density (a slight decrease of A/A before 30 sec is due to geographical curvature of the earth).

As seen in Fig. 1 b), C_m for $X_c = 0.12$ m is close to zero in the free-molecular environments. The pitching moment acting on the capsule is therefore zero in the free-molecular flow, and very small in the transitional flow. Due to these facts, in contrast to the case for $X_c = 0.10$ m, the pitching motion for $X_c = 0.12$ m is little damped even without the initial spin until the aerodynamic force increases, as seen in Fig. 6 b). For $X_c > 0.12$ m, the pitching instability of the capsule becomes significant in the rarefied environments since C_m is positive in the free-molecular conditions (see Fig. 1). When the initial spin is not given to stabilize the capsule, A/A increases to approximately 40 deg. for $X_c = 0.125$ m, while the capsule tumbles during reentry for $X_c = 0.13$ m, as seen in Figs. 6 c) and d), respectively.

Although the pitching instability appears for $X_c > 0.12$ m in the rarefied flight environments, the pitching motion of the capsule can be well stabilized by initiating the spin at a frequency of 0.1 Hz, as shown in Figs. 6 c) and d). The reason for such a low frequency required to achieve the pitching stability is that the magnitude of C_m remains small when $C_m > 0$, and that the moment of inertia about the center axis is large (0.221 kg·m^2) compared with the capsule diameter (0.404 m). Although there remain uncertainties in damping rates of spin and roll motion, they are not expected to make significant influences on the results since these damping rates are considered to be very small in the rarefied environments. From the results described above, the dynamic stability of the MUSES-C capsule is assured in the rarefied environments along the flight trajectory for currently possible positions of the center of gravity, which are $X_c = 0.10$ to 0.13 m and tested in the present study, provided that the spin at a frequency higher than 0.1 Hz is initially given to the capsule.

5. SUMMARY

The aerodynamic coefficients of the MUSES-C sample return capsule were revied from the continuous to free-molecular environments. The transitional aerodynamic coefficients were

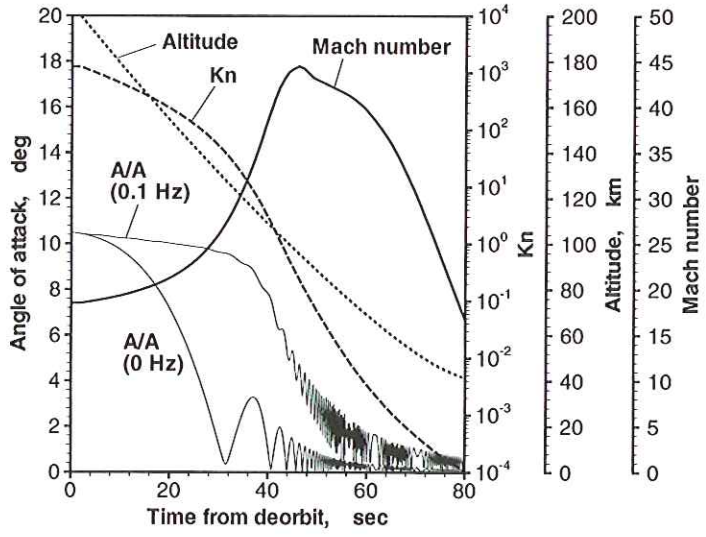

a) $X_c = 0.100$ m

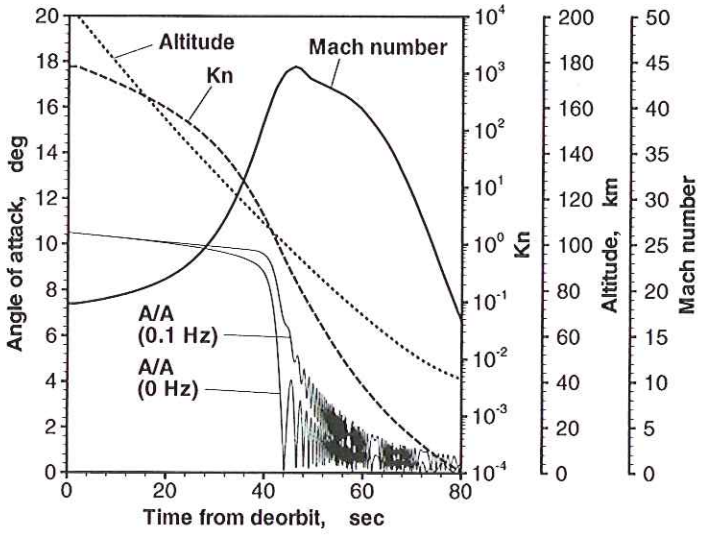

b) $X_c = 0.120$ m

Fig. 6: Evolution of angle of attack along the flight trajectory.

determined by the empirical sine-squared bridging formula, using the values of the continuous and free-molecular aerodynamic coefficients. In order to validate the accuracy of the empirical aerodynamic coefficients in the transitional regime, rarefied flows around the capsule were computed in the three-dimensional geometry by the DSMC method, taking into account the nonequilibrium thermal relaxation and chemical kinetics. The results show that the basic sine-squared bridging formula can be a good approximation to obtain the transitional aerodynamic coefficients for the MUSES-C capsule.

In order to assess the dynamic stability of the capsule during reentry, the 6-degrees-of-freedom dynamics of the MUSES-C capsule was numerically analyzed in the free-molecular to continuous flight environments along the reentry trajectory. Time evolution of the angle of

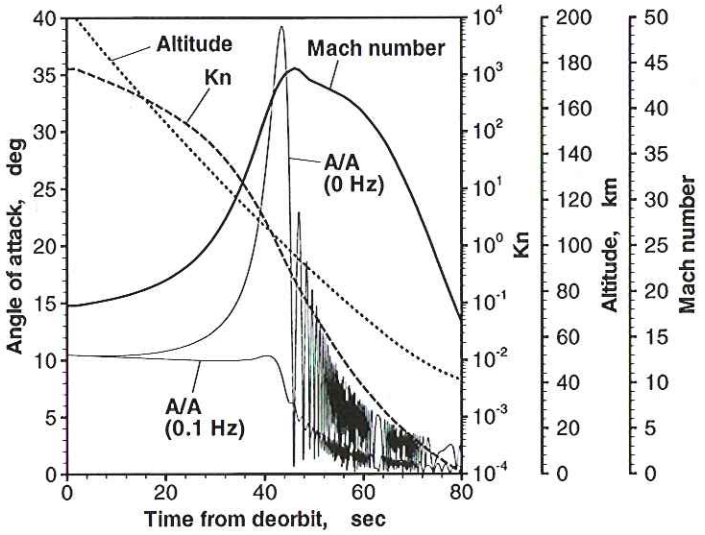

c) $X_c = 0.125$ m

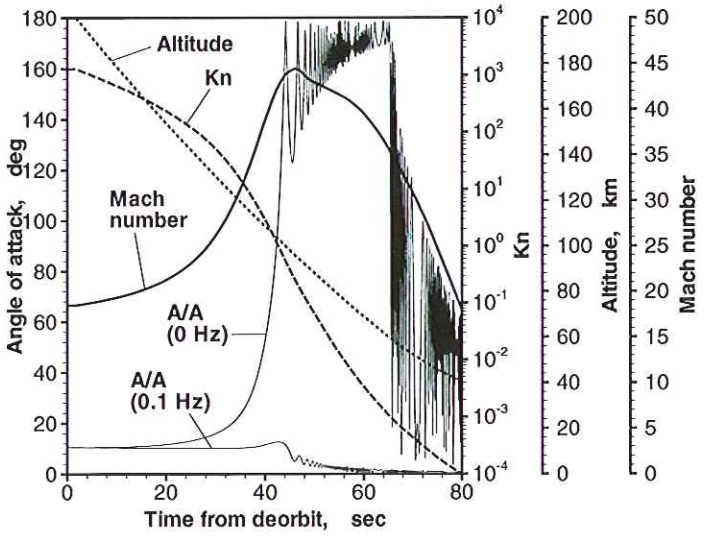

d) $X_c = 0.130$ m

Fig. 6: *Continued.*

attack in the transitional regime is found to depend significantly on the position of the center of gravity when the initial spin is not given to the capsule. Although the pitching instability appears for $X_c > 0.12$ m in the rarefied flight environments, the pitching motion of the capsule is found to be stabilized well by initiating the spin at a frequency of 0.1 Hz for $X_c < 0.13$ m.

REFERENCES

Wilmoth, R.G., Mitcheltree, R.A. and Moss, J.N., 1997, Low-Density Aerodynamics of the Stardust Sample Return Capsule, AIAA Paper, AIAA 97–2510.

Hiraki, K., 2002, The Aerodynamic Data Base for Asteroid Sample Return Capsule, in this bound volume, pp. 343–361.

Blanchard, R.C. and Buck, G.M., 1986, Rarefied-Flow Aerodynamics and Thermosphere Structure from Shuttle Flight Measurements, J. Spacecraft, **23**(1), pp. 18–24.
Bird, G.A., 1981, Monte-Carlo Simulation in an Engineering Context, in Progress in Astronautics and Aeronautics, **74**, Part I, AIAA, New York, pp. 239–255.
Capitelli, M., Gorse, C., Longo, S. and Giordano, D., 1998, Transport Propeties of High Temperature Air Spacies AIAA Paper, 98–2936.
Nanbu, K., 1990, Variable Hard-sphere Model for Gas Mixture, J. Phys. Soc. Japan, **39**(12), pp. 4331–4333.
Boyd, I.D., 1990, Analysis of Rotational Nonequilibrium in Standing Shock Waves of Nitrogen, AIAA J., **28**(1), pp. 1997–1999.
Parker, J.G., 1959, Rotational and Vibrational Relaxation in Diatomic Gases, Phys. Fluids, **2**(4), pp. 449–462.
Lumpkin III, F.E., Chapman, D.R., and Park, C., 1989, A New Rotational Relaxation Model for Use in Hypersonic Computational Fluid Mechanics AIAA Paper, 89–1737
Fujita, K. and Abe, T., 2002, State-to-state Nonequilibrium Rotational Kinetics of Nitrogen behind a Strong Shock Wave, AIAA Paper, 2002–3217.
Park, C., 1993, Review of Chemical-Kinetic Problems of Future NASA Missions, I: Earth Entries J. Thermophysics and Heat Transfer, **7**(3), pp. 385–398.
Borgnakke, C. and Larsen, P.S., 1975, Statistical Collision Model for Monte Carlo simulation of Polyatomic Gas Mixture, J. Compt. Phys., **18**, pp. 405–420.
Bird, G.A., 1979, Simulation of Multi-dimensional and Chemically Reacting Flows in Rarefied Gas Dynamics, **1**, CEA, Paris, pp. 365–388.
Boyd, I.D., 1990, Rotational-translational Energy Transfer in Rarefied Nonequilibrium Flows, Phys. Fluids A, **2**(3), pp. 447–452.
Nanbu, K., 1992, DSMC techniques for Boltzmann Equation, in Computational Fluid Dynamics (in Japanese), Hohara, M. and Omiya, H. ed., 1992, University of Tokyo Press, Tokyo, Chap. 13, pp. 287–319.
Justus, C.G., Jeffries III, W.R., Yung, S.P. and Johnson, D.L., 1995, The NASA/MSFC Global Reference Atmosphere Model–1995 Version (GRAM95), NASA TM–4715.